Siri et al. *Boundary Value Problems* (2018) 2018:126
https://doi.org/10.1186/s13661-018-1019-6

Boundary Value Problems
a SpringerOpen Journal

RESEARCH Open Access

Heat transfer over a steady stretching surface in the presence of suction

Zailan Siri[1*], Nor Artisham Che Ghani[1] and Ruhaila Md. Kasmani[2]

*Correspondence:
zailansiri@um.edu.my
[1]Institute of Mathematical Sciences, Faculty of Science, University of Malaya, Kuala Lumpur, Malaysia
Full list of author information is available at the end of the article

Abstract

The purpose of this paper is to present the Cattaneo–Christov heat flux model for Maxwell fluid past a stretching surface where the presence of suction/injection is taken into account. The governing system of equations is reduced to the ordinary differential equations with the boundary conditions by similarity transformation. These equations are then solved numerically by two approaches, Haar wavelet quasilinearization method (HWQM) and Runge–Kutta–Gill method (RK Gill). The behavior of various pertinent parameters on velocity and temperature distributions is analyzed and discussed. Comparison of the obtained numerical results is made between both methods and with the existing numerical solutions found in the literature, and reasonable agreement is noted.

Keywords: Cattaneo–Christov heat flux; Maxwell fluid; Haar wavelet quasilinearization method; Runge–Kutta–Gill method; Suction/injection

1 Introduction

The phenomenon of heat transfer exists due to the difference in temperature between objects or between different parts of the same object. The well-known heat conduction law, known as Fourier's law, proposed by Fourier [1] provides an insight into the heat transfer analysis. However, this law causes a parabolic energy equation, which means that any initial disturbance is instantly felt through the medium under consideration. Due to this obstacle, Cattaneo [2] revised this law by adding a relaxation time term. Later, Christov [3] made some modification on the Cattaneo model by replacing the ordinary derivative with Oldroyd's upper-convected derivative. This model is recognized as Cattaneo–Christov heat flux model in the literature. Straughan [4] studied thermal convection in a horizontal layer of incompressible Newtonian fluid by using the Cattaneo–Christov model. Ciarletta and Straughan [5] proved the uniqueness and stability of solutions for the Cattaneo–Christov equations. By using the Cattaneo–Christov model, Tibullo and Zampoli [6] studied the uniqueness of solutions for incompressible fluid.

The Maxwell fluid model is one of the simplest viscoelastic models that can address the influence of fluid relaxation time. Due to these reasons, this model has received remarkable attention of researchers. Han *et al.* [7] employed the upper-convected Maxwell (UCM) model and Cattaneo–Christov heat flux model to investigate the heat transfer and boundary layer flow of viscoelastic fluid above a stretching plate with velocity slip boundary by using homotopy analysis method (HAM). Mustafa [8] also used HAM to investigate

the rotating flow of UCM fluid through the Cattaneo–Christov heat flux model. Khan *et al*. [9] studied the boundary layer flow of UCM fluid induced by an exponentially stretching sheet using the Cattaneo–Christov model. Hayat *et al*. [10] discussed the impact of Cattaneo–Christov heat flux in the flow over a stretching sheet with variable thickness.

Abbasi *et al*. [11] investigated the Cattaneo–Christov heat flux model for a two-dimensional laminar boundary layer flow of incompressible Oldroyd-B fluid over a linearly stretching sheet, where the dimensionless velocity and temperature profiles are obtained through the optimal homotopy analysis method (OHAM). Mushtaq *et al*. [12] studied the Sakiadis flow of Maxwell fluid along a moving plate in calm fluid by considering the Cattaneo–Christov model. Abbasi and Shehzad [13] proposed a mathematical model to study the Cattaneo–Christov heat flux model for the three-dimensional flow of Maxwell fluid over a bi-directional stretching surface by employing the homotopic procedure. Rubab and Mustafa [14] used HAM to investigate the magnetohydrodynamic (MHD) three-dimensional flow of UCM fluid over a bi-directional stretching surface.

Related to this presence, Vajravelu [15] analyzed the convection flow and heat transfer of viscous fluid near an infinite, porous, and vertical stretching surface by using variable size finite difference method. Muthucumaraswamy [16] studied the effects of suction on heat and mass transfer along a moving vertical surface in the presence of chemical reaction. El-Arabawy [17] investigated the effects of suction/injection and chemical reaction on mass transfer over a stretching surface. Elbashbeshy and Bazid [18] analyzed the effect of internal heat generation and suction or injection on the heat transfer in a porous medium over a stretching surface. Sultana *et al*. [19] discussed the effects of internal heat generation, radiation, and suction or injection on the heat transfer in a porous medium over a stretching surface. Rajeswari *et al*. [20] studied the effect of chemical reaction, heat, and mass transfer on a nonlinear MHD boundary layer flow through a vertical porous surface with heat source in the presence of suction. Elbashbeshy *et al*. [21] used the Runge–Kutta technique to study the effects of suction/injection and variable chemical reaction on mass transfer characteristics over the unsteady stretching surface embedded in a porous medium.

In view of all the above mentioned literature and to the best of our knowledge, no attempt has been made so far to study suction/injection on a Maxwell fluid flow past a steady stretching surface. Motivated by this, our aim here is to analyze the effects of a suction/injection parameter on Maxwell fluid by considering the Cattaneo–Christov heat flux model. The governing system of partial differential equations is non-dimensionalized [22–24] and transformed into the ordinary differential equations and solved numerically by employing the HWQM and RK Gill method. Comparisons are made with the available results in a limiting manner. The effects of involved parameters on the velocity and temperature fields are analyzed and discussed.

The rest this paper is organized as follows. Section 2 is devoted to the mathematical formulation of the flow problem including the reduced ordinary differential equations. In Sect. 3, the numerical solutions of HWQM and RK Gill are shown. Numerical results and discussion are presented in Sect. 4. Finally, the conclusion is given in Sect. 5.

2 Mathematical formulation

Consider a laminar boundary layer two-dimensional flow of incompressible, upper-convected Maxwell fluid past a stretching surface with the presence of suction/injection. The heat transfer process is studied through the Cattaneo–Christov heat flux theory. In

the absence of the gradient of pressure, the governing equations expressing conservation of mass, momentum, and energy are given as follows:

$$\frac{\partial u}{\partial x}+\frac{\partial v}{\partial y}=0, \tag{1}$$

$$u\frac{\partial u}{\partial x}+v\frac{\partial u}{\partial y}+\lambda_1\left(u^2\frac{\partial^2 u}{\partial x^2}+v^2\frac{\partial^2 u}{\partial y^2}+2uv\frac{\partial^2 u}{\partial x\,\partial y}\right)=\nu\frac{\partial^2 u}{\partial y^2}, \tag{2}$$

$$\begin{aligned}u\frac{\partial T}{\partial x}+v\frac{\partial T}{\partial y}+\lambda_2\Bigg(&u\frac{\partial u}{\partial x}\frac{\partial T}{\partial x}+v\frac{\partial v}{\partial y}\frac{\partial T}{\partial y}+u\frac{\partial v}{\partial x}\frac{\partial T}{\partial y}+v\frac{\partial u}{\partial y}\frac{\partial T}{\partial x}+2uv\frac{\partial^2 T}{\partial x\,\partial y}\\&+u^2\frac{\partial^2 T}{\partial x^2}+v^2\frac{\partial^2 T}{\partial y^2}\Bigg)=\alpha\frac{\partial^2 T}{\partial y^2},\end{aligned} \tag{3}$$

where u and v denote the velocity components along the x- and y-directions, respectively. ν is the kinematic viscosity, λ_1 is the fluid relaxation time, λ_2 is the thermal relaxation time, T is the temperature of Maxwell fluid, and $\alpha = k/\rho c_p$ is thermal diffusivity, where k is the thermal conductivity.

The boundary conditions in the present problem are

$$\begin{aligned}&u=ax, \qquad v=v_0, \qquad T=T_w \quad \text{at } y=0\\&u\to 0, \qquad T\to T_\infty \quad \text{as } y\to\infty.\end{aligned} \tag{4}$$

In the above equation, v_0 represents the velocity of suction/injection at the wall, T_w is the temperature at the wall, and T_∞ is the ambient fluid temperature.

By using these transformations, we have

$$\eta=\sqrt{\frac{a}{\nu}}y, \qquad \psi=\sqrt{\nu a}xf(\eta), \qquad \theta=\frac{T-T_\infty}{T_w-T_\infty}, \tag{5}$$

in which ψ is the stream function, equations (2) and (3) can be reduced to a system of two coupled ordinary differential equations as follows:

$$f'''-f'^2+ff''+\beta\left(2ff'f''-f^2f'''\right)=0 \tag{6}$$

and

$$\frac{1}{\Pr}\theta''+f\theta'-\gamma\left(ff'\theta'+f^2\theta''\right)=0, \tag{7}$$

where the prime denotes the derivative with respect to η. The Prandtl number is given as $\Pr = \nu/\alpha$, where v is the velocity component along y-direction and α is thermal diffusivity. $\beta = \lambda_1 a$ is the Deborah number and $\gamma = \lambda_2 a$ is the non-dimensional thermal relaxation time, where a is a positive constant, λ_1 is fluid relaxation time, and λ_2 is thermal relaxation time. The boundary conditions for equations (6) and (7) are

$$\begin{aligned}&f=s, \qquad f'=1, \qquad \theta=1 \quad \text{at } \eta=0,\\&f'\to 0, \qquad \theta\to 0 \quad \text{as } \eta\to\infty,\end{aligned} \tag{8}$$

where $s=-\frac{v_0}{\sqrt{cv}}$ is a suction parameter and c is a positive constant. Note that $s>0$ corresponds to suction, $s<0$ corresponds to injection, and $s=0$ is an impermeable surface.

3 Numerical solutions

This section presents the numerical solutions of two approaches for solving two coupled nonlinear ODEs (6) and (7), namely

(a) Haar wavelet quasilinearization method (HWQM) and

(b) Runge–Kutta–Gill method (RK Gill)

3.1 Haar wavelet quasilinearization method (HWQM)

This subsection presents the Haar wavelet and quasilinearization approach based scheme for two coupled ordinary differential equations (6) and (7) with boundary conditions (8). Wavelet methods are one of the relatively new techniques for obtaining approximate solutions of differential equations. Commonly used wavelet schemes are Haar wavelets, Legendre wavelets, and Chebyshev wavelets. Among them, we are more interested in Haar wavelet because it is the simplest possible wavelet with a compact support, which means that it vanishes outside of a finite interval. In numerical analysis, the discovery of compactly supported wavelets has proven to be a useful tool for the approximation of functions.

The Haar wavelet family for $[0,\tau)$ is defined as [25]

$$h_i(\eta)=\begin{cases}1 & \frac{k\tau}{2^\alpha}\le\eta<\frac{(k+1/2)\tau}{2^\alpha},\\ -1 & \frac{(k+1/2)\tau}{2^\alpha}\le\eta<\frac{(k+1)\tau}{2^\alpha},\\ 0 & \text{elsewhere in } [0,\tau),\end{cases} \tag{9}$$

where $i=1,2,\dots,m-1$ is the series index number and the resolution $m=2^J$ is a positive integer. α and k represent the integer decomposition of the index i, i.e., $i=2^\alpha+k$, in which $\alpha=0,1,\dots,J-1$ and $k=0,1,\dots,2^\alpha-1$.

In the Haar wavelet method, the following integrals are used:

$$p_{i,1}(\eta)=\int_0^\eta h_i\bigl(\eta'\bigr)\,d\eta',\qquad p_{i,\nu+1}(\eta)=\int_0^\eta h_{i,\nu}\bigl(\eta'\bigr)\,d\eta',\quad \nu=1,2,3,\dots. \tag{10}$$

The generalized Haar wavelet and its integration are derived, which could cater the Haar series expansion domain greater than one. This is because the boundary layer fluid flow problem deals with a sufficiently large number of infinite intervals.

Any function $f(\eta)$ square, which is integrable in the interval $[0,\tau)$, can be expressed in the following form of Haar wavelets:

$$f(\eta)=\sum_{i=0}^{m-1}c_ih_i(\eta), \tag{11}$$

where the Haar coefficients c_i can be obtained from

$$c_i=\frac{2^\alpha}{\tau}\int_0^\tau f(\eta)h_i(\eta)\,d\eta. \tag{12}$$

The above series terminates at finite terms if $f(\eta)$ is a piecewise constant or can be approximated as a piecewise constant during each subinterval.

There are several possibilities for treating the nonlinearity in BVPs. However, here the well-known technique quasilinearization [26] is used to tackle the nonlinearity in equations (6) and (7). A simple procedure for numerical calculations is introduced for easy understanding [27, 28]. The nonlinear ODEs (6) and (7) followed by quasilinearization lead to

$$\alpha_{1,r} f'''_{r+1} + \alpha_{2,r} f''_{r+1} + \alpha_{3,r} f'_{r+1} + \alpha_{4,r} f_{r+1} = R_1, \tag{13}$$

$$\beta_{1,r} f'_{r+1} + \beta_{2,r} f_{r+1} + \beta_{3,r} \theta''_{r+1} + \beta_{4,r} \theta'_{r+1} = R_2, \tag{14}$$

where r is the number of iteration, and

$$\alpha_{1,r} = 1 - \beta f_r^2, \qquad \alpha_{2,r} = f_r + 2\beta f_r f'_r, \qquad \alpha_{3,r} = -2f'_r + 2\beta f_r f''_r,$$

$$\alpha_{4,r} = \frac{1}{1-\beta f_r^2}\left(-2\beta f_r f'^2_r + f''_r + \beta f_r^2 f''_r + 2\beta f'_r f''_r + 2\beta^2 f_r^2 f'_r f''_r\right),$$

$$\beta_{1,r} = -\Pr \gamma f_r \theta'_r, \qquad \beta_{2,r} = \frac{\Pr \theta'_r}{1 - \Pr \gamma f_r^2}\left(1 + \Pr \gamma f_r^2 - \gamma f'_r\right),$$

$$\beta_{3,r} = 1 - \Pr \gamma f_r^2, \qquad \beta_{4,r} = \Pr f_r \left(1 - \gamma f'_r\right),$$

$$R_1 = f'_r\left(-f'_r + 2\beta f_r f''_r\right) + \frac{\beta f_r}{1-\beta f_r^2}\left(-2f_r f'^2_r + \frac{1}{\beta} f''_r + f_r^2 f''_r + 2f'_r f''_r + 2\beta f_r^2 f'_r f''_r\right),$$

$$R_2 = -\Pr \gamma f_r f'_r \theta'_r + \frac{\Pr \theta'_r f_r}{1 - \Pr \gamma f_r^2}\left(1 + \Pr \gamma f_r^2 - \gamma f'_r - \Pr \gamma^2 f_r^2 f'_r\right).$$

The boundary conditions are

$$\begin{aligned} &f_{r+1} = s, \qquad f'_{r+1} = 1, \qquad \theta_{r+1} = 1 \quad \text{at } \eta = 0, \\ &f'_{r+1} \to 0, \qquad \theta_{r+1} \to 0 \quad \text{as } \eta \to \infty. \end{aligned} \tag{15}$$

Now, we apply the Haar wavelet method to (13) and (14), then approximate the higher order derivative term by Haar wavelet series as follows [29, 30]:

$$f'''_{r+1}(\eta) = \sum_{i=0}^{m-1} a_i h_i(\eta) \tag{16}$$

and

$$\theta''_{r+1}(\eta) = \sum_{i=0}^{m-1} b_i h_i(\eta), \tag{17}$$

respectively. The lower order derivatives are obtained by integrating (16) and (17) and using the boundary conditions

$$f''_{r+1}(\eta) = \sum_{i=0}^{m-1} a_i \left(p_{i,1}(\eta) - \frac{1}{L} p_{i,2}(L)\right) - \frac{1}{L}, \tag{18}$$

$$f'_{r+1}(\eta) = \sum_{i=0}^{m-1} a_i \left(p_{i,2}(\eta) - \frac{\eta}{L} p_{i,2}(L)\right) - \frac{\eta}{L} + 1, \tag{19}$$

$$f_{r+1}(\eta) = \sum_{i=0}^{m-1} a_i \left(p_{i,3}(\eta) - \frac{\eta^2}{2L} p_{i,2}(L) \right) - \frac{\eta^2}{2L} + \eta + s, \tag{20}$$

$$\theta'_{r+1}(\eta) = \sum_{i=0}^{m-1} b_i \left(p_{i,1}(\eta) - \frac{1}{L} p_{i,2}(L) \right) - \frac{1}{L}, \tag{21}$$

$$\theta_{r+1}(\eta) = \sum_{i=0}^{m-1} b_i \left(p_{i,2}(\eta) - \frac{\eta}{L} p_{i,2}(L) \right) - \frac{\eta}{L} + 1, \tag{22}$$

where L is a sufficiently large number. Substitute equations (18)–(22) and higher order derivatives into equations (13) and (14). By applying discretization on equations (13) and (14) and using the collocation points $x_c = \frac{(c+0.5)\tau}{m}$, $c = 0, 1, \ldots, m-1$, we obtain the following systems:

$$\sum_{i=0}^{m-1} a_i K_1 = L_1, \tag{23}$$

$$\sum_{i=0}^{m-1} a_i K_2 + \sum_{i=0}^{m-1} b_i K_3 = L_2, \tag{24}$$

where

$$\begin{aligned}
K_1 &= \left(1 - \beta f_r^2\right) h_i(\eta) - 2\left(f'_r - \beta f_r f''_r\right) p_{i,2}(\eta) - f_r\left(-1 - 2\beta f'_r\right) p_{i,1}(\eta) \\
&\quad - \frac{2}{L}\left(-\eta f'_r + \beta \eta f_r f''_r + \frac{1}{2} f_r + \beta f_r f'_r \right) p_{i,2}(L) - \frac{1}{1 - \beta f_r^2} \\
&\quad \times \left[2\beta \left(f_r f'^2_r - \frac{1}{2\beta} f''_r - \frac{1}{2} f_r^2 f''_r - f'_r f''_r - \beta f_r^2 f'_r f''_r \right) p_{i,3}(\eta) \right. \\
&\quad \left. + \frac{\beta}{2L} \eta \left(-2\eta f_r f'^2_r + \frac{1}{\beta} \eta f''_r + \eta f_r^2 f''_r + 2\eta f'_r f''_r + 2\beta \eta f_r^2 f'_r f''_r \right) p_{i,2}(L) \right], \\
K_2 &= \Pr \gamma f_r \theta'_r \left(-p_{i,2}(\eta) + \frac{1}{L} \eta p_{i,2}(L) \right) + \frac{1}{1 - \Pr \gamma f_r^2} \left[\frac{\Pr}{2L} \eta^2 \theta'_r \left(-1 - \Pr \gamma f_r^2 \right. \right. \\
&\quad \left. \left. + \gamma f'_r + \Pr \gamma^2 f_r^2 f'_r \right) p_{i,2}(L) + \Pr \theta'_r \left(1 + \Pr \gamma f_r^2 - \gamma f'_r - \Pr \gamma^2 f_r^2 f'_r \right) p_{i,3}(\eta) \right], \\
K_3 &= \left(1 - \Pr \gamma f_r^2\right) h_i(\eta) + \Pr f_r \left(1 - \gamma f'_r\right) p_{i,1}(\eta) + \frac{\Pr}{L} f_r \left(-1 + \gamma f'_r\right) p_{i,2}(L), \\
L_1 &= \frac{2\beta}{L} \left(-\frac{L}{2\beta} f'^2_r + L f_r f'_r f''_r - \frac{1}{\beta} \eta f'_r + \frac{L}{\beta} f'_r + \eta f_r f''_r - L f_r f''_r + \frac{1}{2\beta} f_r + f_r f'_r \right) \\
&\quad + \frac{1}{1 - \beta f_r^2} \left[2\beta \left(-f_r^2 f'^2_r + \frac{1}{2\beta} f_r f''_r + \frac{1}{2} f_r^3 f''_r \right. \right. \\
&\quad \left. + f_r f'_r f''_r + \beta f_r^3 f'_r f''_r + s f_r f'^2_r - \frac{1}{2\beta} s f''_r - s f'_r f''_r - \beta s f_r^2 f'_r f''_r - \frac{1}{2} s f_r^2 f''_r \right) \\
&\quad + \frac{\beta}{2L} \eta \left(-2\eta f_r f'^2_r + 4L f_r f'^2_r + \frac{1}{\beta} \eta f''_r + \eta f_r^2 f''_r \right. \\
&\quad \left. \left. - 2L f_r^2 f''_r + 2\eta f'_r f''_r - 4L f'_r f''_r + 2\beta \eta f_r^2 f'_r f''_r - 4\beta L f_r^2 f'_r f''_r - \frac{2L}{\beta} f''_r \right) \right],
\end{aligned}$$

$$
\begin{aligned}
L_2 = {} & \frac{\Pr\gamma}{L} f_r \left(-L f_r' \theta_r' + \frac{1}{\gamma} - f_r' - \eta\theta_r' + L\theta_r' \right) \\
& + \frac{1}{1-\Pr\gamma f_r^2} \Big[\Pr\theta_r' \big(\Pr\gamma f_r^3 + f_r - \gamma f_r f_r' - \Pr\gamma^2 f_r^3 f_r' - s \\
& - \Pr\gamma s f_r^2 + \gamma s f_r' + \Pr\gamma^2 s f_r^2 f_r' \big) \\
& + \frac{\Pr}{2L} \eta\theta_r' \big(\eta - 2L + \Pr\gamma\eta f_r^2 - 2L\Pr\gamma f_r^2 - \gamma\eta f_r' + 2L\gamma f_r' \\
& - \Pr\gamma^2 \eta f_r^2 f_r' + 2L\Pr\gamma^2 f_r^2 f_r' \big) \Big].
\end{aligned}
$$

Equations (23) and (24) can be solved simultaneously to obtain Haar coefficients a_i and b_i. We choose the initial approximations which satisfy the boundary conditions (15) as follows:

$$f_0(\eta) = s + \left(1 - \mathrm{e}^{-\eta}\right) \tag{25}$$

and

$$\theta_0(\eta) = \mathrm{e}^{-\eta}. \tag{26}$$

Then we put the Haar coefficients in equations (20) and (22) to find the approximate solutions.

As our work is based on the quasilinearization technique and Haar wavelet method, so the convergence for both schemes can be seen in literature [31, 32].

3.2 Runge–Kutta–Gill method (RK Gill)

The nonlinear ordinary differential equations (6)–(7) subject to the boundary conditions (8) are of the third order in f and of the second order in θ. These equations are numerically solved by employing the fourth-order Runge–Kutta–Gill method integrated with shooting technique and Newton–Raphson method. We define

$$f = Y_1, \qquad f' = Y_2, \qquad f'' = Y_3, \qquad \theta = Y_4, \qquad \theta' = Y_5. \tag{27}$$

We also define the following:

$$f' = F_1, \qquad f'' = F_2, \qquad f''' = F_3, \qquad \theta' = F_4, \qquad \theta'' = F_5. \tag{28}$$

Substitute equations (27) and (28) into equations (6)–(7), these equations are reduced to a system of nine simultaneous equations of the first order as follows:

$$F_1 = Y_2, \tag{29}$$

$$F_2 = Y_3, \tag{30}$$

$$F_3 = Y_2^2 - Y_1 Y_3 - \beta\left(2Y_1 Y_2 Y_3 - Y_1^2 F_3\right), \tag{31}$$

$$F_4 = Y_5, \tag{32}$$

$$F_5 = \Pr\left[-Y_1 Y_5 + \gamma\left(Y_1 Y_2 Y_5 + Y_1^2 F_5\right)\right]. \tag{33}$$

The boundary conditions given in (8) are replaced by

$$Y_1(0) = s, \qquad Y_2(0) = 1, \qquad Y_4(0) = 1, \tag{34}$$

$$Y_2(\eta_\infty) = 0, \qquad Y_4(\eta_\infty) = 0. \tag{35}$$

Here, η_∞ is selected to vary from 5 to 7, depending on the set of the physical parameters. The unknown initial conditions are denoted by $Y_3(0) = \zeta$ and $Y_5(0) = t$. We use the Newton–Raphson method to find ζ and t such that the solutions of equations (29)–(35) satisfy the outer boundary condition (8). In this case, we start with the initial estimate values $(\zeta^{(0)}, t^{(0)})$ by the shooting method. The Newton–Raphson algorithm is expanded to include partial derivatives with respect to each variable's dimension. This would yield the derivative of $\boldsymbol{F}(F_1, F_2, \ldots, F_5)$ with respect to ζ and t as follows:

$$\boldsymbol{F}_\zeta(F_6, F_7, \ldots, F_{10}), \qquad \boldsymbol{F}_t(F_{11}, F_{12}, \ldots, F_{15}). \tag{36}$$

Thus, we need to find $\boldsymbol{F}_\zeta = 0, \boldsymbol{F}_t = 0$, simultaneously. Following Cebeci and Keller [33], this yields a system of algebraic equations which satisfy the boundary conditions when $\eta \to \infty$:

$$f'_\zeta \zeta + f'_t t + f' = 0, \qquad \theta_\zeta \zeta + \theta_t t + \theta = 0. \tag{37}$$

Rearranging the system in equation (37) yields a matrix equation $AX = B$:

$$\begin{bmatrix} f'_\zeta & f'_t \\ \theta_\zeta & \theta_t \end{bmatrix} \begin{bmatrix} \zeta \\ t \end{bmatrix} = \begin{bmatrix} -f' \\ -\theta \end{bmatrix}. \tag{38}$$

This matrix equation can be solved by Cramer's rule. The next approximation of ζ and t can be computed by using the following formula:

$$\zeta^{(\text{new})} = \zeta^{(\text{old})} + \frac{\det(A_B(I,J))}{\det(A)}, \qquad t^{(\text{new})} = t^{(\text{old})} + \frac{\det(A_B(I,J))}{\det(A)}. \tag{39}$$

Once the values of ζ and t are known, we use the fourth-order Runge–Kutta–Gill method to solve the first order of ordinary differential equations $F_1, F_2, \ldots, F_{15}$. Following Gill [34], the Runge–Kutta formula is

$$\begin{aligned} Y_{i+1} &= Y_i + \frac{1}{6}hk_1 + \frac{1}{3}\left(\frac{2-\sqrt{2}}{2}\right)hk_2 + \frac{1}{3}\left(\frac{2+\sqrt{2}}{2}\right)hk_3 + \frac{1}{6}hk_4, \\ k_1 &= F(Y_i), \\ k_2 &= F(Y_i + h/2k_1), \\ k_1 &= F(Y_i + (2-\sqrt{2}/2k_1 + (2-\sqrt{2}/2k_2), \\ k_1 &= F(Y_i - \sqrt{2}/2hk_2 + (2+\sqrt{2}/2k_3), \end{aligned} \tag{40}$$

where h is denoted as the stepsize. In the present work, the stepsize of $h = 0.01$ is found to be satisfactory in obtaining the numerical solutions. For convergence, the maximum

Table 1 Comparison of local Nusselt number $-\theta'(0)$ in the case of Newtonian fluid ($\beta = \gamma = b = f_w = 0$) for different values of Pr

Pr	Wang [35]	Gorla and Sidawi [36]	Khan and Pop [37]	Malik *et al.* [38]	HWQM	RK Gill
0.70	0.4539	0.5349	0.4539	0.45392	0.453930	0.453917
2.00	0.9114	0.9114	0.9113	0.91135	0.911345	0.911358
7.00	1.8954	1.8905	1.8954	1.89543	1.895489	1.895403
20.0	3.3539	3.3539	3.3539	3.35395	3.353905	3.353904

Table 2 The values of $-\theta'(0)$ and $-f''(0)$ when Pr = 1 and $s = 0$

γ	$-f''(0)$						$-\theta'(0)$					
	$\beta = 0.1$		$\beta = 0.15$		$\beta = 0.2$		$\beta = 0.1$		$\beta = 0.15$		$\beta = 0.2$	
	RK Gill	HWQM	RK Gill	HWQM	RK Gill	HWQM	RK Gill	HWQM	RK Gill	HWQM	RK Gill	HWQM
0.1	1.02654	1.02653	1.03940	1.03939	1.05215	1.05214	0.58379	0.58379	0.57983	0.57983	0.57593	0.57593
0.4							0.61014	0.61014	0.60553	0.60554	0.60101	0.60101
0.5							0.61998	0.61998	0.61516	0.61516	0.61042	0.61042
0.6							0.63029	0.63029	0.62526	0.62526	0.62031	0.62031
0.8							0.65215	0.65215	0.64673	0.64673	0.64138	0.64138
1.0							0.67551	0.67551	0.66972	0.66972	0.66400	0.66400

absolute relative difference between two iterations is employed within a pre-assigned tolerance $\varepsilon <= 10^{-5}$. If the difference meets the convergence criteria, the solution is assumed to have converged and the iterative process is terminated.

4 Results and discussion

The transformed momentum equation (6) and energy equation (7) subjected to the boundary conditions of equation (8) were numerically solved by means of HWQM and RK Gill method. The computations for HWQM and RK Gill were performed by using MATLAB.

The elasticity number is important for viscoelastic materials. If $\beta < 1$, it corresponds to the fluids, thus a smaller elasticity number ($\beta < 1$) characterizes purely viscous behavior of fluids. On the contrary, for $\beta > 1$, the fluid behaves like elastically solid material. Due to this, the magnitude of velocity is larger in smaller β fluid. By using HWQM, the value of $f''(0)$ in the case of $\beta = 1$ is -1.24178, while $\theta'(0)$ is -0.55244 at $\gamma = 0.6$.

Table 1 depicts the validation of the present results by comparing them with the published results under some special and limited case where the elasticity number ($\beta = 0$) and heat flux relaxation time ($\gamma = 0$) with different values Pr. A favorable agreement is found between these results.

Table 2 shows the values of $f''(0)$ and $\theta'(0)$ for various values of heat flux relaxation parameter γ and elasticity number β. The values computed through both methods are found in favorable agreement. Table 2 indicates that the surface friction coefficient $f''(0)$ decreases with the increase in the values of elasticity number. At any value of γ, there is no effect of changing in the value of heat flux relaxation because equation (6) does not have a direct impact on γ. This table also shows that the value of the surface temperature $\theta'(0)$ decreases with the increase in heat flux relaxation, but it tends to increase with the enhanced elasticity number, which is opposite to the effect on the surface friction coefficient.

Additionally, Table 3 is tabulated for examining the surface friction coefficient and surface temperature gradient for different values of suction/injection parameter s and elastic-

Table 3 The values of $-f''(0)$ and $-\theta'(0)$ for different values of β and s when Pr = 1 and $\gamma = 0.5$

s	$-f''(0)$						$-\theta'(0)$					
	$\beta = 0.1$		$\beta = 0.15$		$\beta = 0.2$		$\beta = 0.1$		$\beta = 0.15$		$\beta = 0.2$	
	RK Gill	HWQM	RK Gill	HWQM	RK Gill	HWQM	RK Gill	HWQM	RK Gill	HWQM	RK Gill	HWQM
−1.0	0.59681	0.59764	–	0.58640	–	0.57485	0.14996	0.16047	–	0.16116	–	0.16186
−0.6	0.73250	0.73351	0.72619	0.72733	0.72004	0.72106	0.29747	0.29864	0.29721	0.29825	0.29673	0.29788
−0.3	0.86492	0.86440	0.86510	0.86508	0.86570	0.86568	0.43848	0.43362	0.43370	0.43161	0.42215	0.42964
0	1.02654	1.02653	1.03940	1.04003	1.05215	1.05271	0.61998	0.61998	0.61516	0.61516	0.61042	0.61061
0.2	1.15770	1.15770	1.18362	1.18361	1.21115	1.20962	0.79129	0.79129	0.78417	0.78417	0.77714	0.77715
0.3	1.23124	1.23064	1.26593	1.26542	1.30242	1.30056	0.89857	0.89891	0.88998	0.89024	0.88119	0.88164
0.6	1.48751	1.48644	1.56384	1.56195	–	1.64070	1.37559	1.37604	1.35999	1.36049	–	1.34471

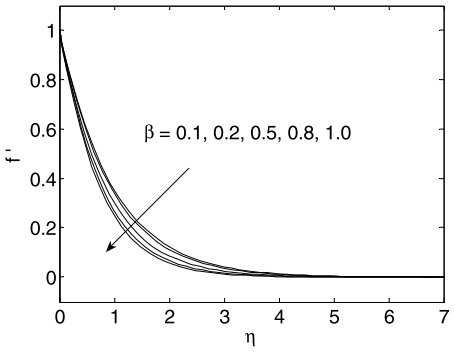

Figure 1 The velocity profile for different values of β when Pr = 1, $\gamma = 0.5$, and $s = 0$

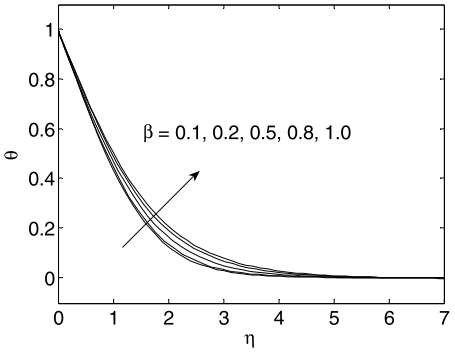

Figure 2 The temperature profile for different values of β when Pr = 1, $\gamma = 0.5$, and $s = 0$

ity number β. These tables clearly present that $f''(0)$ and $\theta'(0)$ are reduced as the parameter of s increases.

Figures 1 and 2 show the effects of elasticity number β on the velocity and temperature distributions. The elastic force disappears when $\beta = 0$ and the fluid becomes Newtonian fluid. From Fig. 1, it is clear that with the increase of β, the velocity distribution shows decreasing behavior. Physically, higher β indicates stronger viscous force which restricts the fluid motion, and subsequently the velocity decreases. Characteristics of β on the temperature distribution are displayed in Fig. 2. Temperature distribution increases for large values of β. The increased parameter of β corresponds to larger relaxation time, which provides resistance to the fluid motion, and as a result more heat is produced. Therefore, temperature distribution increases.

The impact of non-dimensional heat flux relaxation time γ on temperature can be explained through Fig. 3. Temperature distribution is a decreasing function of thermal re-

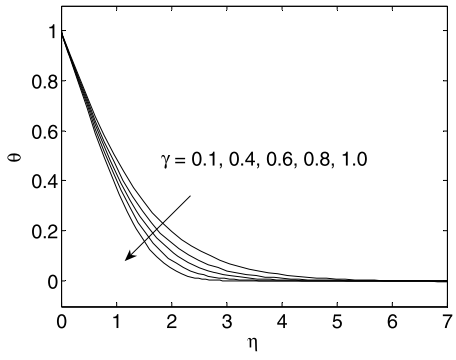

Figure 3 The temperature profile for different values of γ when Pr = 1, $\beta = 0.2$, and $s = 0$

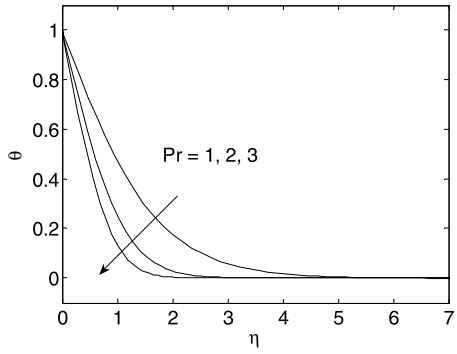

Figure 4 The temperature profile for different values of Pr when $\beta = 0.1$, $\gamma = 0.2$, and $s = 0$

laxation parameter. It is also analyzed that thermal boundary layer thickness decreases. This is due to the fact that as the thermal relaxation parameter increases, particles of the material require more time to transfer heat to their neighboring particles. In other words, non-conducting behavior showed by the higher values of thermal relaxation parameter material is responsible for reduction of temperature distribution.

Figure 4 represents the temperature profile in response to a change in Pr. The graph depicts that an increase in Pr leads to reduction in temperature and thermal boundary layer thickness. Pr is the ratio of momentum to the thermal diffusivity. The thermal diffusivity is weaker for larger Pr due to the fact that the rate of diffusion decreases. Such reduction in the diffusion rate acts as an agent showing reduction in temperature and thermal boundary layer thickness. Here, we do not show the graph for $f'(\eta)$ since there is no effect of changing Pr. This phenomenon can be roughly observed from equation (6), where Pr is the coefficient of temperature and has a direct impact on temperature. The impact of Pr on velocity is achieved through the coupling of various terms, hence the effect may be weakened.

Figures 5 and 6 show the velocity and temperature profiles with respect to the suction/injection parameter s. The fluid velocity and temperature field are found to decrease with increasing value of s. Suction ($s > 0$) causes the velocity of fluid to decrease in the boundary layer region. This effect acts to decrease the wall shear stress. On the other hand, increase in suction causes progressive thinning of the boundary layer.

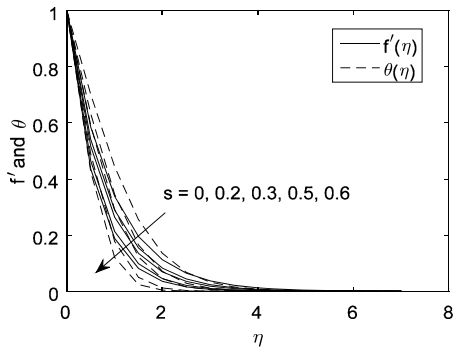

Figure 5 The velocity and temperature profiles for different values of s (impermeable surface and suction) when Pr = 1, $\beta = 0.2$, and $\gamma = 0.5$

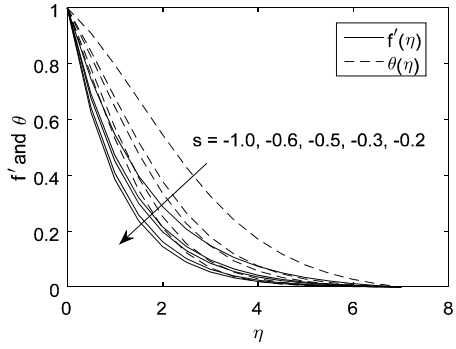

Figure 6 The velocity and temperature profiles for different values of s (injection) when Pr = 1, $\beta = 0.2$, and $\gamma = 0.5$

5 Conclusions

The boundary layer flow of Maxwell fluid past a stretching surface is numerically studied in the presence of suction/injection by using two different methods, namely HWQM and RK Gill. The governing partial differential equations were transformed into a system of ordinary differential equations using similarity transformation before being solved numerically. The impact of elasticity number β, non-dimensional thermal relaxation time γ, suction s, and Prandtl number Pr is examined. The main findings can be summarized as follows:

(a) The elasticity number β has opposite effects on the velocity field and temperature field;

(b) Temperature profile decreases with an increase in Pr and the temperature boundary layer becomes thinner;

(c) Variation of suction/injection parameter s affects both velocity and temperature fields. The larger number of s leads to reduction in velocity and temperature distributions;

(d) $f''(0)$ is found to decrease upon increasing the suction/injection parameter;

(e) No effect of changing the value of heat flux relaxation γ on the surface friction coefficient $f''(0)$ is noticed;

(f) $\theta'(0)$ decreases with the increase in heat flux relaxation, but it tends to increase with the enhanced elasticity number.

Appendix

Proof for equations (6) *and* (7) With ψ as a stream function and the velocity components being given by $u = \partial\psi/\partial y$ and $v = -\partial\psi/\partial x$, the similarity transformation is introduced as in equation (5). Hence, the velocity components and their derivatives can be expressed as follows:

$$u = \frac{\partial}{\partial y}\left(\sqrt{\nu a}xf(\eta)\right) = ax\frac{\partial f}{\partial \eta}, \tag{A1}$$

$$v = -\frac{\partial}{\partial x}\left(\sqrt{a\nu}xf(\eta)\right) = -\sqrt{a\nu}f, \tag{A2}$$

$$\frac{\partial u}{\partial x} = \frac{\partial}{\partial x}\left(ax\frac{\partial f}{\partial \eta}\right) = a\frac{\partial f}{\partial \eta} + ax\frac{\partial^2 f}{\partial x\,\partial \eta}, \tag{A3}$$

$$\frac{\partial u}{\partial y} = \frac{\partial}{\partial y}\left(ax\frac{\partial f}{\partial \eta}\right) = ax\frac{\partial^2 f}{\partial \eta^2}\sqrt{\frac{a}{\nu}}, \tag{A4}$$

$$\frac{\partial^2 u}{\partial x^2} = \frac{\partial}{\partial x}\left(a\frac{\partial f}{\partial \eta} + ax\frac{\partial^2 f}{\partial x\,\partial \eta}\right) = 2a\frac{\partial^2 f}{\partial x\,\partial \eta} + ax\frac{\partial^3 f}{\partial x^2\,\partial \eta}, \tag{A5}$$

$$\frac{\partial v}{\partial y} = \frac{\partial}{\partial y}(-\sqrt{a\nu}f) = -a\frac{\partial f}{\partial \eta}, \tag{A6}$$

$$\frac{\partial v}{\partial x} = \frac{\partial}{\partial x}(-\sqrt{a\nu}f) = -\sqrt{a\nu}\frac{\partial f}{\partial x}, \tag{A7}$$

$$\frac{\partial^2 u}{\partial y^2} = \frac{\partial}{\partial y}\left(ax\frac{\partial^2 f}{\partial \eta^2}\sqrt{\frac{a}{\nu}}\right) = \frac{a^2}{\nu}x\frac{\partial^3 f}{\partial \eta^3}, \tag{A8}$$

$$\frac{\partial^2 u}{\partial x\,\partial y} = \frac{\partial}{\partial x}\left(ax\frac{\partial^2 f}{\partial \eta^2}\sqrt{\frac{a}{\nu}}\right) = a\sqrt{\frac{a}{\nu}}\frac{\partial^2 f}{\partial \eta^2} + a\sqrt{\frac{a}{\nu}}x\frac{\partial^3 f}{\partial x\,\partial \eta^2}. \tag{A9}$$

Substitute all the related derivatives into momentum equation (2). Hence, we will get

$$\begin{aligned}
&a^2x\left(\frac{\partial f}{\partial \eta}\right)^2 + (ax)^2\frac{\partial f}{\partial \eta}\frac{\partial^2 f}{\partial x\,\partial \eta} - a^2xf\frac{\partial^2 f}{\partial \eta^2}\\
&\quad + \lambda_1\left[(ax)^2\left(\frac{\partial f}{\partial \eta}\right)^2\left(2a\frac{\partial^2 f}{\partial x\,\partial \eta} + ax\frac{\partial^3 f}{\partial x^2\,\partial \eta}\right)\right]\\
&\quad + \lambda_1 a^3xf^2\frac{\partial^3 f}{\partial \eta^3} - 2\lambda_1 a^3xf\frac{\partial f}{\partial \eta}\frac{\partial^2 f}{\partial \eta^2} - 2\lambda_1 a^3x^2f\frac{\partial f}{\partial \eta}\frac{\partial^3 f}{\partial x\,\partial \eta^2} = a^2x\frac{\partial^3 f}{\partial \eta^3}.
\end{aligned}$$

Dividing the equation above by a^2x, we get

$$\begin{aligned}
&\frac{\partial^3 f}{\partial \eta^3} - \left(\frac{\partial f}{\partial \eta}\right)^2 + f\frac{\partial^2 f}{\partial \eta^2} + 2\beta f\frac{\partial f}{\partial \eta}\frac{\partial^2 f}{\partial \eta^2} - \beta f^2\frac{\partial^3 f}{\partial \eta^3}\\
&\quad = (ax)^2\frac{\partial f}{\partial \eta}\frac{\partial^2 f}{\partial x\,\partial \eta}\\
&\qquad + \beta\left[ax^2\left(\frac{\partial f}{\partial \eta}\right)^2\left(2a\frac{\partial^2 f}{\partial x\,\partial \eta} + ax\frac{\partial^3 f}{\partial x^2\,\partial \eta}\right)\right] - 2\beta(ax)^2f\frac{\partial f}{\partial \eta}\frac{\partial^3 f}{\partial x\,\partial \eta^2},
\end{aligned} \tag{A10}$$

where $\beta = \lambda_1 a$.

The derivatives for energy equation (3) are given as follows:

$$T = T_\infty + \theta \Delta T, \tag{A11}$$

where $\Delta T = T_w - T_\infty$.

$$\frac{\partial T}{\partial x} = \Delta T \frac{\partial \theta}{\partial x} + \Delta T\left(\frac{\partial \theta}{\partial \eta}\frac{\partial \eta}{\partial x}\right) = \Delta T \frac{\partial \theta}{\partial x}, \tag{A12}$$

$$\frac{\partial^2 T}{\partial x^2} = \frac{\partial}{\partial x}\left(\Delta T \frac{\partial \theta}{\partial x}\right) = \Delta T \frac{\partial^2 \theta}{\partial x^2}, \tag{A13}$$

$$\frac{\partial T}{\partial y} = \Delta T \frac{\partial \theta}{\partial \eta}\frac{\partial \eta}{\partial y} = \Delta T \sqrt{\frac{a}{\nu}}\frac{\partial \theta}{\partial \eta}, \tag{A14}$$

$$\frac{\partial^2 T}{\partial y^2} = \frac{\partial}{\partial y}\left(\Delta T \sqrt{\frac{a}{\nu}}\frac{\partial \theta}{\partial \eta}\right) = \Delta T \frac{a}{\nu}\frac{\partial^2 \theta}{\partial \eta^2}, \tag{A15}$$

$$\frac{\partial^2 T}{\partial x\,\partial y} = \frac{\partial}{\partial x}\left(\frac{\partial T}{\partial y}\right) = \Delta T \sqrt{\frac{a}{\nu}}\frac{\partial^2 \theta}{\partial x\,\partial \eta}. \tag{A16}$$

Thus, energy equation (3) becomes

$$\begin{aligned} &ax\Delta T \frac{\partial f}{\partial \eta}\frac{\partial \theta}{\partial x} - af\Delta T \frac{\partial \theta}{\partial \eta} + \lambda_2 a^2 x \Delta T\left(\frac{\partial f}{\partial \eta}\right)^2 \frac{\partial \theta}{\partial x} + \lambda_2 (ax)^2 \Delta T \frac{\partial f}{\partial \eta}\frac{\partial^2 f}{\partial x\,\partial \eta}\frac{\partial \theta}{\partial x} \\ &\quad + \lambda_2 a^2 \Delta T f \frac{\partial f}{\partial \eta}\frac{\partial \theta}{\partial \eta} - \lambda_2 a^2 x \Delta T \frac{\partial f}{\partial \eta}\frac{\partial f}{\partial x}\frac{\partial \theta}{\partial \eta} - \lambda_2 a^2 x \Delta T \frac{\partial^2 f}{\partial \eta^2}\frac{\partial \theta}{\partial x} \\ &\quad + \lambda_2 (ax)^2 \Delta T\left(\frac{\partial f}{\partial \eta}\right)^2 \frac{\partial^2 \theta}{\partial x^2} + \lambda_2 (af)^2 \Delta T \frac{\partial^2 \theta}{\partial \eta^2} - 2\lambda_2 a^2 x f \Delta T \frac{\partial f}{\partial \eta}\frac{\partial^2 \theta}{\partial x\,\partial \eta} = \alpha \Delta T \frac{a}{\nu}\frac{\partial^2 \theta}{\partial \eta^2}. \end{aligned}$$

Multiplying equation above by $\frac{\nu}{\alpha \Delta T a}$, we get

$$\begin{aligned} &\frac{\partial^2 \theta}{\partial \eta^2} + \mathrm{Pr} f \frac{\partial \theta}{\partial \eta} - \mathrm{Pr}\,\gamma f \frac{\partial f}{\partial \eta}\frac{\partial \theta}{\partial \eta} - \mathrm{Pr}\,\gamma f^2 \frac{\partial^2 \theta}{\partial \eta^2} \\ &\quad = \mathrm{Pr}\, x \frac{\partial f}{\partial \eta}\frac{\partial \theta}{\partial x} + \mathrm{Pr}\,\gamma x\left(\frac{\partial f}{\partial \eta}\right)^2 \frac{\partial \theta}{\partial x} + \mathrm{Pr}\,\gamma x \frac{\partial f}{\partial \eta}\frac{\partial^2 f}{\partial x\,\partial \eta}\frac{\partial \theta}{\partial x} - \mathrm{Pr}\,\gamma x \frac{\partial f}{\partial \eta}\frac{\partial f}{\partial x}\frac{\partial \theta}{\partial \eta} \\ &\qquad - \mathrm{Pr}\,\gamma x \frac{\partial^2 f}{\partial \eta^2}\frac{\partial \theta}{\partial x} + \mathrm{Pr}\,\gamma x\left(\frac{\partial f}{\partial \eta}\right)^2 \frac{\partial^2 \theta}{\partial x^2} - 2\,\mathrm{Pr}\,\gamma x f \frac{\partial f}{\partial \eta}\frac{\partial^2 \theta}{\partial x \partial \eta}, \end{aligned} \tag{A17}$$

where $\mathrm{Pr} = \nu/\alpha$ and $\gamma = \lambda_2 a$.

The new boundary conditions are given as follows:

At $y = 0$, $\eta = y\sqrt{\frac{a}{\nu}} \to \eta = 0$,

$$u = ax, \qquad u = ax\frac{\partial f}{\partial \eta} = ax \to \frac{\partial f}{\partial \eta} = 1, \tag{A18}$$

$$v = v_0, \qquad v = -\sqrt{av} f = v_0 \to f = -\frac{v_0}{\sqrt{av}}, \tag{A19}$$

where $s = -\frac{v_0}{\sqrt{av}}$(suction/injection)

$$T = T_w, \qquad \theta = \frac{T - T_\infty}{T_w - T_\infty} \to \theta = \frac{T_w - T_\infty}{T_w - T_\infty} = 1. \tag{A20}$$

As $y \to \infty, \eta = y\sqrt{\frac{a}{\nu}} \Rightarrow \eta \to \infty$,

$$u \to 0, \quad u = ax\frac{\partial f}{\partial \eta} \Rightarrow \frac{\partial f}{\partial \eta} \to 0, \tag{A21}$$

$$T \to T_\infty, \quad \theta = \frac{T_\infty - T_\infty}{T_w - T_\infty} \Rightarrow \theta \to 0. \tag{A22}$$

From (A10) and (A17), the coordinates x and y are transformed to the independent variables ξ and ψ, where ξ is identical to x and ψ is the stream function. If we replace the partial derivative with respect to ξ in equation (A10) by difference quotients, the resulting difference-differential equation, which only contains derivative with respect to η, can be solved using numerical methods for nonlinear ordinary differential equations. By discretizing both the differential expressions, it can be transformed to a difference equation.

Thus, equations (A10) and (A17) become

$$f''' - f'^2 + ff'' + \beta\left(2ff'f'' - f^2f'''\right) = 0, \tag{A23}$$

$$\frac{1}{\mathrm{Pr}}\theta'' + f\theta' - \gamma\left(ff'\theta' + f^2\theta''\right) = 0, \tag{A24}$$

with boundary conditions

$$f = s, \qquad f' = 1, \qquad \theta = 1 \quad \text{at } \eta = 0 \quad \text{and} \quad f' \to 0, \qquad \theta \to 0 \quad \text{as } \eta \to \infty. \tag{A25}$$

The prime denotes the derivative with respect to η. □

Acknowledgements
The authors would like to thank the Ministry of Higher Education Malaysia and University of Malaya for the financial support (RG397-17AFR).

Funding
University of Malaya Research Grant (RG397-17AFR).

Availability of data and materials
Not applicable.

Competing interests
The authors declare that they have no competing interests.

Authors' contributions
All authors contributed equally and significantly in writing this article. All authors read and approved the final manuscript.

Author details
[1] Institute of Mathematical Sciences, Faculty of Science, University of Malaya, Kuala Lumpur, Malaysia. [2] Mathematics Division, Centre for Foundation Studies in Science, University of Malaya, Kuala Lumpur, Malaysia.

Publisher's Note

Received: 23 January 2018 Accepted: 19 June 2018 Published online: 15 August 2018

References

1. Fourier, J.B.J.: Théorie Analytic. De La Chaleur, Paris (1822)
2. Cattaneo, C.: Sulla conduzione del calore. Atti Semin. Mat. Fis. Univ. Modena Reggio Emilia **3**, 83–101 (1948)
3. Christov, C.I.: On frame indifferent formulation of the Maxwell–Cattaneo model of finite speed heat conduction. Mech. Res. Commun. **36**(4), 481–486 (2009)
4. Straughan, B.: Thermal convection with the Cattaneo–Christov model. Int. J. Heat Mass Transf. **53**(1–3), 95–98 (2010)

5. Ciarletta, M., Straughan, B.: Uniqueness and structural stability for the Cattaneo–Christov equations. Mech. Res. Commun. **37**(5), 445–447 (2010)
6. Tibullo, V., Zampoli, V.: A uniqueness result for the Cattaneo–Christov heat conduction model applied to incompressible fluids. Mech. Res. Commun. **38**(1), 77–79 (2011)
7. Han, S., Zheng, L., Li, C., Zhang, X.: Coupled flow and heat transfer in viscoleastic fluid with Cattaneo–Christov heat flux model. Appl. Math. Lett. **38**, 87–93 (2014)
8. Mustafa, M.: Cattaneo–Christov heat flux model for rotating flow and heat transfer of upper-convected Maxwell fluid. AIP Adv. (2015) https://doi.org/10.1063/1.4917306
9. Khan, J.A., Mustafa, M., Hayat, T., Alsaedi, A.: Numerical study of Cattaneo–Christov heat flux model for viscoelastic flow due to an exponentially stretching sheet. PLoS ONE (2015) https://doi.org/10.1371/journal.pone.0137363
10. Hayat, T., Farooq, M., Alsaedi, A., Al-Solamy, F.: Impact of Cattaneo–Christov heat flux in the flow over a stretching sheet with variable thickness. AIP Adv. (2015) https://doi.org/10.1063/1.4929523
11. Abbasi, F.M., Mustafa, M., Shehzad, S.A., Alhuthali, M.S., Hayat, T.: Analytical study of Cattaneo–Christov heat flux model for a boundary layer flow of Oldroyd-B fluid. Chin. Phys. B (2016) https://doi.org/10.1088/1674-1056/25/1/014701
12. Mushtaq, A., Abbasbandy, S., Mustafa, M., Hayat, T., Alsaedi, A.: Numerical solution for Sakiadis flow of upper-convected Maxwell fluid using Cattaneo–Christov heat flux model. AIP Adv. (2016) https://doi.org/10.1063/1.4940133
13. Abbasi, F.M., Shehzad, S.A.: Heat transfer analysis for three-dimensional flow of Maxwell fluid with temperature dependent thermal conductivity: application of Cattaneo–Christov heat flux model. J. Mol. Liq. **220**, 848–854 (2016)
14. Rubab, K., Mustafa, M.: Cattaneo–Christov heat flux model for MHD three-dimensional flow of Maxwell fluid over a stretching sheet. PLoS ONE (2016) https://doi.org/10.1371/journal.pone.0153481
15. Vajravelu, K.: Convection heat transfer at a stretching sheet with suction or blowing. J. Math. Anal. Appl. **188**(3), 1002–1011 (1994)
16. Muthucumaraswamy, R.: Effects of suction on heat and mass transfer along a moving vertical surface in the presence of a chemical reaction. Forsch. Ingenieurwes. **67**, 129–132 (2002) https://doi.org/10.1007/s10010-002-0083-2
17. El-Arabawy, H.A.M.: Exact solution of mass transfer over a stretching surface with chemical reaction and suction/injection. J. Math. Stat. **5**(3), 159–166 (2009)
18. Elbashbeshy, E.M.A., Bazid, M.A.A.: Heat transfer in a porous medium over a stretching surface with internal heat generation and suction or injection. Appl. Math. Comput. **158**(3), 799–807 (2004)
19. Sultana, T., Saha, S., Rahman, M.M., Saha, G.: Heat transfer in a porous medium over a stretching surface with internal heat generation and suction or injection in the presence of radiation. J. Mech. Eng. **40**(1), 22–28 (2009)
20. Rajeswari, R., Jothiram, B., Nelson, V.K.: Chemical reaction, heat and mass transfer on nonlinear MHD boundary layer flow through a vertical porous surface in the presence of suction. Appl. Math. Sci. **3**(50), 2469–2480 (2009)
21. Elbashbeshy, E.M.A., Emam, T.G., Abdel-wahed, M.S.: Mass transfer over unsteady stretching surface embedded in porous medium in the presence of variable chemical reaction and suction/injection. Appl. Math. Sci. **5**(12), 557–571 (2011)
22. Autuori, G., Cluni, F., Gusella, V., Pucci, P.: Mathematical models for nonlocal elastic composite materials. Adv. Nonlinear Anal. **6**(4), 355–382 (2017)
23. Ghergu, M., Radulescu, V.: Nonlinear PDEs. Mathematical Models in Biology, Chemistry and Population Genetics. Springer Monographs in Mathematics. Springer, Heidelberg (2012)
24. Vallée, C., Radulescu, V., Atchonouglo, K.: New variational principles for solving extended Dirichlet–Neumann problems. J. Elast. **123**(1), 1–18 (2016)
25. Ghani, C.N.A.: Numerical solution of elliptic partial differential equations by Haar wavelet operational matrix method. Dissertation, University of Malaya (2012)
26. Mandelzweig, V.B., Tabakin, F.: Quasilinearization approach to nonlinear problems in physics with application to nonlinear ODEs. Comput. Phys. Commun. **141**, 268–281 (2001)
27. Marin, M., Craciun, E.M.: Uniqueness results for a boundary value problem in dipolar thermoelasticity to model composite materials. Composites, Part B, Eng. **126**, 27–37 (2017)
28. Marin, M., Baleanu, D.: On vibrations in thermoelasticity without energy dissipation for micropolar bodies. Bound. Value Probl. **2016**, 111 (2016) https://doi.org/10.1186/s13661-016-0620-9
29. Lepik, Ü.: Numerical solution of differential equations using Haar wavelets. Math. Comput. Simul. **68**(2), 127–143 (2005)
30. Lepik, Ü.: Numerical solution of evolution equations by the Haar wavelet method. Appl. Math. Comput. **185**(1), 695–704 (2007)
31. Lee, E.S.: Quasilinearization and Invariant Imbedding with Applications to Chemical Engineering and Adaptive Control. Academic Press, New York (1968)
32. Saeed, U., Rehman, M.U.: Haar wavelet-quasilinearization technique for fractional nonlinear differential equations. Appl. Math. Comput. **220**, 630–648 (2013)
33. Cebici, T., Keller, H.: Shooting and parallel shooting methods for solving the Falkner–Skan boundary-layer equation. J. Comput. Phys. **7**(2), 289–300 (1971)
34. Gill, S.: A process for the step-by-step integration of differential equations in an automatic digital computing machine. Math. Proc. Camb. Philos. Soc. **47**(1), 96–108 (1951)
35. Wang, C.Y.: Free convection on a vertical stretching surface. J. Appl. Math. Mech. **69**(11), 418–420 (1989)
36. Gorla, R.S.R., Sidawi, I.: Free convection on a vertical stretching surface with suction and blowing. Appl. Sci. Res. **52**(3), 247–257 (1994)
37. Khan, W.A., Pop, I.: Boundary-layer flow of a nanofluid past a stretching sheet. Int. J. Heat Mass Transf. **53**(11–12), 2477–2483 (2010)
38. Malik, R., Khan, M., Shafiq, A., Mushtaq, M., Hussain, M.: An analysis of Cattaneo–Christov double-diffusion model for sisko fluid flow with velocity slip. Results Phys. **7**, 1232–1237 (2017)